Title: Polymeric nano-encapsulation of curcumin enhances its anti-cancer activity in breast (MDA-MB231) and lung (A549) cancer cells through reduction in expression of HIF-1α and nuclear p65 (Rel A).

Authors: Mohammed N. Khan[1], Yusuf A Haggag[2], Majella E Lane[3], Paul A. McCarron[1] and Murtaza M. Tambuwala*[1].

Short title: Nanotechnology enhances anti-cancer efficacy

Address:

[1]School of Pharmacy and Pharmaceutical Sciences, Saad Centre for Pharmacy and Diabetes, Ulster University, Cromore Road, Coleraine,
Co. Londonderry BT52 1SA, United Kingdom.
[2]Department of Pharmaceutical Technology, Faculty of Pharmacy, University of Tanta, Tanta , Egypt.
[3]UCL School of Pharmacy, 29-39 Brunswick Square, London, WC1N 1AX, United Kingdom.

***Corresponding Author:** Murtaza M. Tambuwala

Address: Y143, School of Pharmacy and Pharmaceutical Sciences, Saad Centre for Pharmacy and Diabetes, Ulster University, Cromore Road, Coleraine, Co. Londonderry BT52 1SA, United Kingdom.

e-mail: m.tambuwala@ulster.ac.uk

Phone: 0044 28 701 24016

Fax: 004428 701 23518

Abstract

Background: The anti-cancer potential of curcumin, a natural NFκβ inhibitor, has been reported extensively in breast, lung and other cancers. *In vitro* and *in vivo* studies indicate that the therapeutic efficacy of curcumin is enhanced when formulated in a nanoparticulate carrier. However, the mechanism of action of curcumin at the molecular level in the hypoxic tumour micro-environment is not fully understood. Hence, the aim of our study was to investigate the mechanism of action of curcumin formulated as nanoparticles in *in vitro* models of breast and lung cancer under a hypoxic micro-environment.

Methods: Biodegradable poly (lactic-co-glycolic acid) PLGA nanoparticles (NP), loaded with curcumin (cur-PLGA-NP), were fabricated using a solvent evaporation technique to overcome solubility issues and to facilitate intracellular curcumin delivery. Cytotoxicity of free curcumin and cur-PLGA-NP were evaluated in MDA-MB-231 and A549 cell lines using migration, invasion and colony formation assays. All treatments were performed under a hypoxic micro-environment and whole cell lysates from controls and test groups were used to determine the expression of HIF-1α and p65 levels using ELISA assays.

Results: A ten-fold increase in solubility, three-fold increase in anti-cancer activity and a significant reduction in the levels of cellular HIF-1α and nuclear p65 (Rel A) were observed for cur-PLGA-NP, when compared to free curcumin.

Conclusion: Our findings indicate that curcumin can effectively lower the elevated levels of HIF-1α and nuclear p65 (Rel A) in breast and lung cancer cells under a hypoxic tumour micro-environment when delivered in nanoparticulate form. This applied means of colloidal delivery could explain the improved anti-cancer efficacy of curcumin and has further potential applications in enhancing the activity of anti-cancer agents of low solubility.

Keyword: nanotechnology, hypoxia, anti-cancer, curcumin, PLGA, intracellular delivery

1. Introduction

Curcumin is a well-known anti-cancer agent found in the rhizomes of the perennial herb *Curcuma longa*. It has a long history of use in traditional medicine, covering a broad spectrum of conditions, such as cancer, diabetes, inflammation and Alzheimer's disease[1, 2]. The FDA has endorsed its status as a safe, home-based remedy. In more structured and rigorous evaluations, comprising of more than 65 clinical trials, curcumin's benefit in life-threatening diseases has been clearly demonstrated[3]. In relation to inflammatory and cancerous disorders, its therapeutic action is attributed to its ability to module nuclear factor kappa-beta (NFκβ) transcriptional factor [4 5] and hypoxia inducible factor (HIF) [6 7]. Free curcumin and curcumin loaded into a nanoparticulate carrier have been reported to be of therapeutic value in almost all cancer types [8 9 10 11]. However, the exact molecular mechanism of action involved in the treatment of cancer under a pathophysiological, hypoxic, tumour micro-environment is not clearly understood. It is known that over activation of NFκβ and HIF pathways is induced by an hypoxic micro-environment, which has been reported extensively in several tumour types [12 13 14, 15]. This hypoxic micro-environment has been deemed responsible for metabolic adaption of cancerous cells, which result in tumour development, progression and reduced effectiveness of cancer therapeutics [14].

Among all cancer types, breast cancer has been reported as the major cause of death among elderly women in Europe and the United States [16 17]. Paclitaxel, 5-flourouracil, cyclosporine and doxorubicin are the most commonly prescribed treatment options for breast and lung cancer [18, 19 & 20]. However, these conventional chemotherapeutics result in serious side-effects, such as constipation, nausea, alopecia, neuronal damage, bone marrow depletion and heart failure [21 22]. Of similar concern is mortality associated with lung cancer, which is reported as the major cause of cancer-related death in males in developing countries. This outcome contributes approximately 18.2% to the total cancer death statistic [23]. Furthermore,

tiredness, skin reactions, loss of appetite, neurotoxicity and hair loss are some of the general side effects associated with conventional therapeutics [24]. Patients suffering from breast and lung cancers usually have to undergo surgery and radiation-based treatments, in addition to chemotherapy. Furthermore, these therapies are not site specific and cause extensive damage to healthy tissue [25]. In addition, these interventions interfere with the menopause and fertility [26]. Hence, there is a pressing need to continue to develop safer and more effective alternatives for treating neoplastic disease.

The therapeutic value of curcumin in the treatment of breast and lung cancer has been reported in *in vitro*, *in vivo* and clinical studies [27,28]. However, these findings highlight problematic solubility issues of curcumin, which result in low systemic bioavailability, poor pharmacokinetic profiles and sub-optimal delivery to target cells [29,30]. Thus, the first objective of the present work was to use emulsion-based encapsulation methods to formulate a drug delivery system for curcumin with improved solubility and intra-cellular delivery properties. Nano-encapsulation of drugs in PLGA matrices has been reported to enhance therapeutic efficacy and targeting capabilities [31], protect from degradation [32] and improve aqueous solubility of poorly water-soluble drugs [33,34]. Since curcumin is practically insoluble in water, it makes an ideal model drug for our current investigation [35]. Nano-encapsulation is also known to enhance cellular permeability and retention effects, which are proposed as mechanisms to target and enhance drug accumulation in solid tumour masses [36]. Since hypoxia plays a critical role in tumour development and progression, the second objective of our work was to investigate the molecular mechanism of action of free curcumin and nano-encapsulated curcumin. Of particular interest was the effect on expression of two master transcriptional regulators HIF-1α and p65 (Rel A), which are known to be expressed in response to hypoxia and are positively associated with almost all cancer types [37,38].

We hypothesise that nano-encapsulation of curcumin will enhance its solubility and facilitate intracellular delivery. These events will result in improved bioavailability and enhanced anti-cancer activity *via* modulation of the over-activated NFκβ and HIF pathways in lung and breast cancer cells seen under hypoxic condition. We hypothesise further that there will be a resultant stabilisation of the tumour, and cessation of cell growth and spread. In this study, the solvent evaporation method was employed, using sonication to homogenise the emulsion phases, and poly(vinyl alcohol) (PVA) to stabilise and control particle size [39]. Optimisations of PLGA and PVA content were carried out to select optimum settings during the formulation of curcumin-loaded PLGA NP (cur-PLGA-NP). The nanoparticle formulation exhibiting superior cellular uptake, retention and *in vitro* release was selected for further assessment of anti-cancer and anti-metastatic activity of curcumin in the highly metastatic breast (MDA-MB-231) and lung cancer (A549) cell lines.

2. Materials and Methods

2.1 Preparation of cur-PLGA NP

Cur-PLGA-NP was formulated using an oil-in-water emulsion technique. PLGA was dissolved in 2.0 ml chloroform, followed by addition of curcumin and sonication at 55 W for 3 minutes (Branson Sonifier W-350, Danbury, CT, USA). Once dissolution was complete, the solution was added to an aqueous solution of 1.5% PVA and sonicated again at 55 W for 3 minutes to form the final o/w emulsion. This was stirred overnight and then centrifuged at 16584*g* for 30 minutes to assist the removal of residual solvents. The nanospheres obtained were washed three times with deionised distilled water. NP were lyophilised for 72 hours

(FreeZone 4.5plus) and stored at 4 °C until further use [40]. Fluorescent NP were prepared by adding 1μg of Nile Red to PLGA/curcumin solution in ethanol. [40]

2.2 Physicochemical characterisation

2.2.1 Particles size and zeta potential

Particle size and distribution of cur-PLGA-NP were determined using dynamic light scattering (Zetasizer 5000, Malvern Instruments, Malvern, UK). An aliquot of NP suspension (5 mg ml^{1}), previously vortex, was diluted in ultrapure water and used to measure mean diameter. Electrophoretic mobility was used to measure the zeta potential of cur-PLGA-NP. Conductivity was adjusted using 0.001 M KCl. The mean of three measurements was recorded [41].

2.2.2 Entrapment efficiency

Entrapment efficiency was determined using an indirect method. The concentration of non-encapsulated curcumin in the supernatant was measured by absorption spectrophotometry at 430 nm and compared to a standard plot [42]. The amount of curcumin encapsulated in NP was calculated from the difference between the initial amount of curcumin added and the non-encapsulated curcumin remaining in the external aqueous phase after NP fabrication. All measurements were recorded in triplicate and the mean of each sample was reported as the percentage of curcumin entrapment efficiency.

2.2.3 In vitro release study

The release of curcumin from PLGA NP was determined in phosphate buffered saline (pH 7.4, containing 0.1% w/v Tween-80) as a release phase. Briefly, cur-PLGA-NP (5.0 mg) were suspended in a dialysis compartment (MW cut-off 17 kD) and suspended in 1.0 ml PBS solution. The sample pouches were incubated at 37 °C in a reciprocal shaking water bath (100 rpm) [35]. Samples were taken during a period of 168 hours at predetermined time intervals.

2.2.4 Determination of water solubility

Apparent water solubility of curcumin, formulated as cur-PLGA-NP, was compared with an equivalent amount of free curcumin dispersed in distilled water. The mixtures were stirred for 24 hours. These solutions were then centrifuged at 13,450*g* for 10 minutes and the absorbance of the supernatant measured using ultraviolet spectroscopy [43].

2..2.5 Particle surface morphology

Surface morphology was characterised using scanning electron microscopy (FEI Quanta 400 FEG, FEI). A sample of NP was mounted on carbon tape and sputter-coated with gold under vacuum in an argon atmosphere prior to imaging.

2.3 Culture materials

MDA-MB-231 cells (a metastatic breast cancer cell line) and A549 cells (a metastatic lung cancer cell line) were maintained as monolayer cultures in Dulbecco's modified Eagle's medium–high glucose (DMEM-Hi) medium (Gibco BRL, Grand Island, NY) supplemented with 10% foetal bovine serum (Gibco BRL, Grand Island, NY) and 1% penicillin–streptomycin (Gibco BRL, Grand Island, NY) at 37 °C in a humidified atmosphere (5% CO2).

Different concentration of free curcumin and cur-PLGA-NP were dissolved in 20 μl of DMSO. This solution was then diluted to 2 ml with Optimem® media.

177

178 **2.4 Co-localisation of cur-PLGA-NP**

179 Cellular uptake of cur-PLGA-NP was investigated by seeding 1.0×10^5 MDA-MB-231 and
180 A549 cells on chamber slides in 6-well plates. Cells were incubated with Nile Red-labelled
181 cur-PLGA-NP for 24 hours and fixed with 4% paraformaldehyde for 15 minutes. The nucleus
182 was stained with 5.0 μg DAPI in 1.0 ml normal media and incubated for 15 minutes [44]. The
183 fluorescence images were obtained using phase contrast microscopy (Nicole Eclipse E400
184 Florescence Microscope, Nikon Y-FL, Japan).

185

186 **2.5 Migration assay**

187 A migration assay was performed using an *in vitro* scratch assay, as previously described [45].
188 To quantify the results captured from photographic images, ImageJ® software was used to
189 measure the width of the scratch at three different points. The degree of closure over 24 hours
190 was calculated using the difference of the scratch width between 0 and 24 hours for each
191 treatment concentration. The degree of scratch closure for each treatment was compared to the
192 degree of closure in the control cells.

193

194 **2.6 In vitro cytotoxicity**

195 Cytotoxicity assays were performed, as previously reported by Kumar *et al*. [46] with minor
196 modifications. MDA-MB-231 and A549 cells (5.0×10^4 cells per well in 500 μl media) were
197 seeded in 24-well plates. The following day, cells were treated with different concentrations
198 of free curcumin or cur-PLGA-NP suspended in Optimem® media. Medium containing
199 equivalent amounts of blank PLGA NP was used as the control. The cytotoxic effect of 10, 20
200 and 30 μM of the free curcumin or cur-PLGA-NP was determined every 24 hours using MTT
201 assay to assess the viability of cancer cells. The treated cells were washed with 500 μL PBS,

then 500 μL of 15% MTT dye solution in complete media was added to each well. The plates were incubated at 37°C and 5% CO2 for an additional 3 hours. The supernatant was discarded and formazan crystals solubilised by adding 500 μL of DMSO. The absorption was measured at 570 nm (reference wavelength 630 nm) in a microplate reader (Fluostar Omega, BMG Lab Tech GMBH, Germany). The anti-proliferative effect of different doses of free curcumin or cur-PLGA-NP treatments was calculated as a percentage of cell growth with respect to the blank NP controls. The absorbance of the untreated cells was set at 100%. All the experiments were repeated three times.

2.7 Invasion assay

The effect of curcumin treatment on invasion of MDA-MB231 and A549 cells was performed as previously described [47]. Transwell® inserts of 8 μm pore size were inserted in 12-well plates (BD Bioscience, San Jose, CA). 135 μl solutions of Matrigel and water (1:1) was placed on these inserts. Cells ($4x10^4$) were seeded in a suspension of 200 μl of serum free media. Subsequently, 100 μl containing 10, 20 and 30 μM of the free curcumin or cur-PLGA-NP suspended in serum free media was added in the insert. The same volume of 100 μl containing equivalent amounts of blank PLGA NP was used as a control. 700 μl of DMEM media containing 10% FBS was added to each well as chemo-attractant. After 24 hours, the media in both chambers was removed and clean off any remaining cells or Matrigel® layer. The inserts were placed into another well containing 500 μl methanol for 10 minutes for fixation and left to dry. The membrane was cut and placed with the surface facing upwards in wells of a new 12-well plate. Crystal Violet solution (250 μl) was added in the well to stain up the invaded cells. After drying the membrane 250 μl of 70% ethanol was added to membrane and shaken for 30 minutes. 200 μl was pipetted out from this 70% ethanol and absorbance was measured at 590 nm (Fluostar Omega, BMG Lab Tech GMBH, Germany). The effect of different doses

of free curcumin or cur-PLGA-NP treatments was calculated as a percentage of cell invasions with respect to the blank NP controls. The absorbance of the untreated the absorbance of the untreated cells was set at 100%. All the experiments were repeated three times.

2.8 Colony formation assay

An aliquot of approximately 500 cells (MDA-MB-231 and A549) were seeded in 2.0 ml media in 6-well plates and allowed stand for 2 days to attach and initiate colony formation [35]. These cells were treated with different concentrations of 10, 20 and 30 μM of free curcumin or cur-PLGA-NP suspended in Optimem® media over a period of 7 days. The plates were washed twice with PBS, fixed in chilled methanol, stained with Crystal Violet, washed with water and air-dried. The number of colonies was counted visually. The % colony formation was calculated by comparing the number of colonies formed in the test experiment to the number of colonies formed using blank PLGA NP.

2.9 Quantification of HIF-1α and p65 levels

MDA-MB-231 and A549 cells (treated for 24 hours with 10% oxygen) were treated with (i) free curcumin, (ii) cur-PLGA-NP and (iii) blank PLGA-NP. Whole cell lysates were prepared and assayed for HIF-1α and p65 levels using Invitrogen HIF1A Human ELISA Kit (EHIF1A) and NFκβ p65 (Total) Human ELISA Kit (KHO0371) and used according to the manufacturer's instructions at 450 nm, using a BioTek optical plate reader. Optical density was converted to concentration (pg ml^{-1}) using the standard calibration curve provided in the manufacture's protocol.

2.10 Statistical analysis

Each experiment was performed in triplicate. Statistical analysis was performed using GraphPad Prism v5.0. Results are presented as mean +/- standard error of the mean (SEM). Particle size, zeta potential, entrapment efficiency and values of *in vitro* release profiles were treated statistically using one-way analysis of variance (ANOVA). $P < 0.05$ was considered statistically significant.

3. Results and Discussion

3.1 Effect of PLGA concentration

Three batches nanoparticles (F1, F2 and F3) were formulated with a different amount of PLGA and an equal amount of curcumin, as shown in the table I. The effect of increasing the quantity of polymer for the formulation of cur-PLGA-NP on its physiochemical properties is shown in Figure 1. It was found that particle size increased significantly from 265 nm to 606 nm (P-value < 0.0001) as the quantity of PLGA increased (Figure 1A). This increase in size is due to increase in the viscosity of polymer solution and formation of larger disperses droplets [41, 48]. It was also observed that increasing the amount of polymer increased the zeta potential significantly from –13.7 mV (F1) to -3.1 mV (Figure 1B; P-value < 0.01). This could be due to the accumulation of ionised carboxylic groups on the nanoparticles as result of an increase of PLGA. Entrapment efficiency increased significantly, as the ratio of PLGA increased (Figure 1C). Similar results were reported by Derman *et al*. [49]. It is proposed that the increase in PLGA in the organic phase increases the viscosity and reduces diffusivity to the water phase [41, 50]. The data in Figure 1D show the release profile for curcumin from three different

formulations. All three formulations show a similar release trend with a burst effect after 24 hours.

3.2 Solubility of cur-PLGA-NP and free curcumin

The apparent water solubility of curcumin in both free and nano-encapsulated form was determined by UV spectroscopy at 430 nm. The vials in Figure 2A give a visual representation of the enhanced solubility of curcumin when formulated as cur-PLGA-NP when compared to free curcumin in water. It is evident that cur-PLGA-NP produce a uniform dispersion, whereas free curcumin was sparingly soluble in water. The solubility of free curcumin was found to be 0.935 μmol, whereas ostensible solubility of cur-PLGA-NP (curcumin encapsulated in NP) was 9.535 μmol. These results indicate an approximately ten-fold increase in aqueous solubility of cur-PLGA-NP as compared to free curcumin.

3.3 Scanning Electron Microscopy

Figure 3 shows SEM images of F1, F2, and F3 formulated with 30 mg, 60 mg and 90 mg of polymer with equal amounts of curcumin and PVA. F1 exhibits a monodisperse appearance, with the smallest particle size. SEM images of cur-PLGA-NP suggest that an increase in the polymer (PLGA) concentration not only leads to an increase in particle size but also results in non-spherical particles. Thus, F1 batch was selected for *in vitro* analysis based on its smaller particle size.

3.4 Cellular uptake

The nuclei of MDA-MB-231 and A549 cells were stained with DAPI and Nile Red-tagged cur-PLGA-NP were observed under fluorescent microscopy. Cellular uptake of cur-PLGA-NP labelled with Nile Red, in MDA-MB-231 and A549 cells, were visualised by overlaying images

obtained by fluorescent microscopy. Nile Red encapsulated cur-PLGA-NP can be seen within the MDA-MB-231 and A549 cells as depicted in the Figure 4A and 4B. The result indicates that formulation F1 NP may be taken up by the cells. However, since the cell boundaries are not seen clearly this result cannot be confirmed.

3.5 Migration assay

Migration of cancer cells from the primary tumour site to other sites is a predominant feature of metastatic breast and lung cancer cells [51]. Therefore, in this work, a scratch assay was conducted on both cell lines to investigate doses response of free curcumin and cur-PLGA-NP on the migration of MDA-MB-231 (Figure 5A) and A549 (Figure 5B) cells. Figure 5 shows the graphical quantification of the degree of closure in breast and lung cancer cell lines relative to the blank NP controls. Treatment with free curcumin resulted in higher degree of wound closure for all concentrations in both cell lines. Treatment with cur-PLGA-NP resulted in significant reduction in the degree of wound closure compared to the free curcumin after 72 hours at similar concentrations of curcumin (Figure 5A and B). These results demonstrated that cur-PLGA-NP have the superior anti-migration capability when compared to free curcumin.

3.6 Invasion assay

An invasion assay was conducted to investigate the effect of free curcumin and cur-PLGA-NP on the invasion capability of MDA-MB-231 (Figure 6A) and A549 (Figure 6B) cells. Dissemination of tumour cells from the primary site to distant locations starts with cell detachment followed by the local invasion of the normal tissues adjacent to the tumour which then can infiltration through the lymphatic drainage system [51]. Treatment with cur-PLGA-NP resulted in a significant decrease in cell invasion compared to free curcumin for all

concentrations in both cell lines as shown in Figure 6. These results suggest that Cur-PLGA-NP can significantly inhibit the invasion capability of invasive lung and breast cancer cells when compared to free curcumin. This enhanced anti-invasive effect imparted to curcumin by nano-encapsulation is critical to inhibit metastasis of highly invasive breast and lung cancer cells.

3.7 Colony formation assay

Colony formation assay has been widely to study the long-term anti-cancer activity of curcumin[35]. The number of colonies formed after 7 days was quantified for MDA-MB-231 (Figure 7A) and A549 (Figure 7B) cells treated with blank PLGA-NP as control, along with three different concentrations of free curcumin and cur-PLGA-NP. Treatment with cur-PLGA-NP resulted in significantly lower numbers of colonies compared to free curcumin, as shown Figure 7A and B.

3.8 Assessment of HIF-1α and p65 levels

Having assessed the physical parameters, aqueous solubility, intracellular uptake and anti-cancer potential of cur-PLGA-NP versus free curcumin, we need to investigate the molecular mechanism for improved anti-cancer potential of curcumin when formulated as PLGA nanoparticles. Recent research indicates that metastatic human cancer tumours are hypoxic and these cells could have elevated levels HIF-1α and NFκβ/p65 (Rel A) which may result in tumour development and progression of cancer [52] [53-56]. Hence, to investigate if curcumin treatment has an effect on these transcription factors, we used whole cell lysates from metastatic breast (MDA-MB-231) and lung (A549) cancer cells treated with blank NP, cur-PLGA-NP and free curcumin under hypoxic condition (10% O_2) to quantify the levels of HIF-1α and p65 (Rel A) using ELISA assay. The results from the ELISA assay indicated that free

curcumin had no significant effect on the levels of HIF-1α and p65 (Rel A) when compared to blank NP. However, there was a significant reduction in the levels of HIF-1α (Figure 8: Panel A) and p65 (Rel A) (Figure 8: Panel B) in both breast and lung cancer cells treated with cur-PLGA-NP (Figure 8; ($P < 0.001 – 0.01$). These findings indicate that curcumin can suppress the cellular levels of HIF-1α and p65 (Rel A) only when delivered using a colloidal carrier. Metastatic breast (MDA-MB-231) and lung (A549) cancer cells show basal levels of HIF-1α and NFκβ/p65 (Rel A) under normal (21%) atmospheric O_2 level (Supplementary Figure 1).

4. Conclusions

Curcumin has received considerable attention as a potent anti-cancer [57] and anti-inflammatory agent [5]. However, it is not currently used as a clinical medicine for treating inflammation or cancer. Results from our work have demonstrated the effect of increasing amount of PLGA on particle size, zeta potential, entrapment efficiency and *in vitro* release. These findings are in agreement with previously published data [58]. Figure 1 shows that increase in PLGA amount increases the particle size, zeta potential and entrapment efficiency significantly. However, the percentage release decreased with increases in PLGA concentration in the nanoparticle formulation. This may be due to increase in the viscosity of polymer solution. We also observed a ten-fold increase in curcumin solubility when formulated as PLGA nanoparticles (Figure 2) this increased solubility can increase the bioavailability of curcumin and intra-cellular delivery[59]. SEM images from the batches F1, F2 and F3, as shown in Figure 3, demonstrated that increasse in PLGA amount not only leads to increases in particle size, but also distorts the spherical structure of the nanoparticles. Our work indicates that curcumin uptake by cancer cells is achieved when it is formulated as PLGA nanoparticles (Figure 4). This evidence of cellular uptake of curcumin nanoparticles forms the basis of our further findings indicating reduced migration (Figure 5), and proliferation (Supplementary Figure 2) ability decreased invasion power (Figure 6), with reduction in colony formation (Figure 7) of the breast and lung cancer cells. Similar findings related to the anti-cancer potential of curcumin and curcumin nanoparticles have been reported by several researchers [60-67]. However, there is no study to date reporting the action of curcumin and curcumin nanoparticles on elevated levels HIF-1α and p65 (Rel A) in breast and lung cancer cells under tumour hypoxic condition.

The most important findings of our current work indicate that nano-encapsulation of curcumin is capable of downregulating the expression of HIF-1α and p65 (Rel A) levels in

breast and lung cancer cells when exposed to hypoxia (10% O_2) (Figure 8). This finding suggests that the increased therapeutic value of the natural anti-cancer agent curcumin could be via suppression of over activated HIF and NFκβ pathways, which are predominately responsible for adaptation of hypoxic tumours resulting in the development and spread of cancer in our body. Hence, the findings from our work conclude that nanotechnology-based drug delivery system could be an effective tool to enhance the anti-cancer activity of several natural and/or novel anti-cancer compounds, which are currently not in clinical use due to their low solubility and/or poor bioavailability. Future work will involve functionalising these PLGA-NP using salic acid to selectively target cancer tumour cells in *in-vivo* models of lung and breast cancer.

Acknowledgements: We would like to thank Ulster University for providing funding in from of Research Challenge Fund - 2014 for conducting this research project.

Conflict of interest: The authors declare no conflict of interest.

References

1. Naksuriya O, Okonogi S, Schiffelers RM, et al. Curcumin nanoformulations: A review of pharmaceutical properties and preclinical studies and clinical data related to cancer treatment. Biomaterials 2014;35:3365-3383.
2. Prasad S, Gupta SC, Tyagi AK, et al. Curcumin, a component of golden spice: From bedside to bench and back. Biotechnology Advances 2014;32:1053-1064.
3. Yallapu MM, Jaggi M, Chauhan SC. Curcumin Nanomedicine: A Road to Cancer Therapeutics. Curr Pharm Des 2013;19:1994-2010.
4. Thangapazham RL, Sharad S, Maheshwari RK. Skin regenerative potentials of curcumin. Biofactors 2013;39:141-9.
5. Tambuwala MM. Natural Nuclear Factor Kappa Beta Inhibitors: Safe Therapeutic Options for Inflammatory Bowel Disease. Inflamm Bowel Dis 2016;22:719-23.
6. Birner P, Schindl M, Obermair A, et al. Overexpression of hypoxia-inducible factor 1α is a marker for an unfavorable prognosis in early-stage invasive cervical cancer. Cancer Res 2000;60:4693-4696.
7. Bae MK, Kim SH, Jeong JW, et al. Curcumin inhibits hypoxia-induced angiogenesis via down-regulation of HIF-1. Oncol Rep 2006;15:1557-62.
8. Bisht S, Feldmann G, Soni S, et al. Polymeric nanoparticle-encapsulated curcumin ("nanocurcumin"): a novel strategy for human cancer therapy. J Nanobiotechnology 2007;5:3.
9. Bondi ML, Emma MR, Botto C, et al. Biocompatible Lipid Nanoparticles as Carriers To Improve Curcumin Efficacy in Ovarian Cancer Treatment. J Agric Food Chem 2017;65:1342-1352.
10. Kamble S, Utage B, Mogle P, et al. Evaluation of Curcumin Capped Copper Nanoparticles as Possible Inhibitors of Human Breast Cancer Cells and Angiogenesis: a Comparative Study with Native Curcumin. AAPS PharmSciTech 2016;17:1030-41.
11. Xing Z-H, Wei J-H, Cheang T-Y, et al. Bifunctional pH-sensitive Zn (II)–curcumin nanoparticles/siRNA effectively inhibit growth of human bladder cancer cells in vitro and in vivo. Journal of Materials Chemistry B 2014;2:2714-2724.
12. Tafani M, Pucci B, Russo A, et al. Modulators of HIF1α and NFkB in Cancer Treatment: Is it a Rational Approach for Controlling Malignant Progression? Frontiers in Pharmacology 2013;4:13.
13. Redell MS, Tweardy DJ. Targeting transcription factors for cancer therapy. Curr Pharm Des 2005;11:2873-2887.
14. Eales KL, Hollinshead KE, Tennant DA. Hypoxia and metabolic adaptation of cancer cells. Oncogenesis 2016;5:e190.
15. Mimeault M, Batra SK. Hypoxia-inducing factors as master regulators of stemness properties and altered metabolism of cancer- and metastasis-initiating cells. J Cell Mol Med 2013;17:30-54.
16. Chakravarty G, Mathur A, Mallade P, et al. Nelfinavir targets multiple drug resistance mechanisms to increase the efficacy of doxorubicin in MCF-7/Dox breast cancer cells. Biochimie.
17. Malvezzi M, Carioli G, Bertuccio P, et al. European cancer mortality predictions for the year 2016 with focus on leukemias. Ann Oncol 2016;26.
18. Mastro L, Levaggi A, Michelotti A, et al. 5-Fluorouracil, epirubicin and cyclophosphamide versus epirubicin and paclitaxel in node-positive early breast cancer: a phase-III randomized GONO-MIG5 trial. Breast Cancer Res Treat 2015;155:117-126.

19. Zhong Y, Goltsche K, Cheng L, et al. Hyaluronic acid-shelled acid-activatable paclitaxel prodrug micelles effectively target and treat CD44-overexpressing human breast tumor xenografts in vivo. Biomaterials 2016;84:250-261.
20. Gladkov O, Moiseyenko V, Bondarenko IN, et al. Phase II dose-finding study of balugrastim in breast cancer patients receiving myelosuppressive chemotherapy. Med Oncol 2015;32:015-0623.
21. Hanai A, Ishiguro H, Sozu T, et al. Effects of a self-management program on antiemetic-induced constipation during chemotherapy among breast cancer patients: a randomized controlled clinical trial. Breast Cancer Res Treat 2016;155:99-107.
22. Lancellotti P, Anker SD, Donal E, et al. EACVI/HFA Cardiac Oncology Toxicity Registry in breast cancer patients: rationale, study design, and methodology (EACVI/HFA COT Registry)—EURObservational Research Program of the European Society of Cardiology. European Heart Journal - Cardiovascular Imaging 2015;16:466-470.
23. Ridge CA, McErlean AM, Ginsberg MS. Epidemiology of Lung Cancer. Seminars in Interventional Radiology 2013;30:93-98.
24. Landesman-Milo D, Ramishetti S, Peer D. Nanomedicine as an emerging platform for metastatic lung cancer therapy. Cancer Metastasis Rev 2015;34:291-301.
25. Pouw B, de Wit-van der Veen LJ, Stokkel MP, et al. Heading toward radioactive seed localization in non-palpable breast cancer surgery? A meta-analysis. J Surg Oncol 2015;111:185-91.
26. Recio-Saucedo A, Gerty S, Foster C, et al. Information requirements of young women with breast cancer treated with mastectomy or breast conserving surgery: A systematic review. The Breast 2016;25:1-13.
27. Coleman DT, Soung YH, Surh YJ, et al. Curcumin Prevents Palmitoylation of Integrin beta4 in Breast Cancer Cells. PLoS One 2015;10.
28. Kang JH, Kang HS, Kim IK, et al. Curcumin sensitizes human lung cancer cells to apoptosis and metastasis synergistically combined with carboplatin. Exp Biol Med 2015;240:1416-25.
29. Ireson C, Orr S, Jones DJ, et al. Characterization of metabolites of the chemopreventive agent curcumin in human and rat hepatocytes and in the rat in vivo, and evaluation of their ability to inhibit phorbol ester-induced prostaglandin E2 production. Cancer Res 2001;61:1058-64.
30. Ireson CR, Jones DJ, Orr S, et al. Metabolism of the cancer chemopreventive agent curcumin in human and rat intestine. Cancer Epidemiol Biomarkers Prev 2002;11:105-11.
31. Danhier F, Ansorena E, Silva JM, et al. PLGA-based nanoparticles: An overview of biomedical applications. Journal of Controlled Release 2012;161:505-522.
32. Kumari A, Yadav SK, Yadav SC. Biodegradable polymeric nanoparticles based drug delivery systems. Colloids and Surfaces B: Biointerfaces 2010;75:1-18.
33. Brigger I, Dubernet C, Couvreur P. Nanoparticles in cancer therapy and diagnosis. Adv Drug Deliv Rev 2002;54:631-51.
34. Haggag YA, Faheem AM. Evaluation of nano spray drying as a method for drying and formulation of therapeutic peptides and proteins. Frontiers in Pharmacology 2015;6:140.
35. Yallapu MM, Gupta BK, Jaggi M, et al. Fabrication of curcumin encapsulated PLGA nanoparticles for improved therapeutic effects in metastatic cancer cells. J Colloid Interface Sci 2010;351:19-29.
36. Reddy LH. Drug delivery to tumours: recent strategies. J Pharm Pharmacol 2005;57:1231-42.

37. Weichert W, Boehm M, Gekeler V, et al. High expression of RelA/p65 is associated with activation of nuclear factor-kappaB-dependent signaling in pancreatic cancer and marks a patient population with poor prognosis. Br J Cancer 2007;97:523-30.
38. Vaughan DA, Vaughan LN, Stull HD. Dietary modifications of cold-induced metabolic effects. Metabolism 1966;15:781-6.
39. Sahoo SK, Panyam J, Prabha S, et al. Residual polyvinyl alcohol associated with poly (d,l-lactide-co-glycolide) nanoparticles affects their physical properties and cellular uptake. Journal of Controlled Release 2002;82:105-114.
40. Mukerjee A, Vishwanatha JK. Formulation, characterization and evaluation of curcumin-loaded PLGA nanospheres for cancer therapy. Anticancer Res 2009;29:3867-75.
41. Haggag Y, Abdel-Wahab Y, Ojo O, et al. Preparation and in vivo evaluation of insulin-loaded biodegradable nanoparticles prepared from diblock copolymers of PLGA and PEG. International Journal of Pharmaceutics 2016;499:236-246.
42. Bisht S, Feldmann G, Soni S, et al. Polymeric nanoparticle-encapsulated curcumin ("nanocurcumin"): a novel strategy for human cancer therapy. J Nanobiotechnology 2007;5:3.
43. Kim TH, Jiang HH, Youn YS, et al. Preparation and characterization of water-soluble albumin-bound curcumin nanoparticles with improved antitumor activity. Int J Pharm 2011;403:285-91.
44. Lamichhane SP, Arya N, Ojha N, et al. Glycosaminoglycan-functionalized poly-lactide-co-glycolide nanoparticles: synthesis, characterization, cytocompatibility, and cellular uptake. Int J Nanomedicine 2015;10:775-89.
45. Liang C-C, Park AY, Guan J-L. In vitro scratch assay: a convenient and inexpensive method for analysis of cell migration in vitro. Nat. Protocols 2007;2:329-333.
46. Kumar SSD, Mahesh A, Mahadevan S, et al. Synthesis and characterization of curcumin loaded polymer/lipid based nanoparticles and evaluation of their antitumor effects on MCF-7 cells. Biochimica et Biophysica Acta (BBA)-General Subjects 2014;1840:1913-1922.
47. Yuen HF, Gunasekharan VK, Chan KK, et al. RanGTPase: a candidate for Myc-mediated cancer progression. J Natl Cancer Inst 2013;105:475-88.
48. Cui F, Cun D, Tao A, et al. Preparation and characterization of melittin-loaded poly (DL-lactic acid) or poly (DL-lactic-co-glycolic acid) microspheres made by the double emulsion method. J Control Release 2005;107:310-9.
49. Derman S. Caffeic Acid Phenethyl Ester Loaded PLGA Nanoparticles: Effect of Various Process Parameters on Reaction Yield, Encapsulation Efficiency, and Particle Size. Journal of Nanomaterials 2015;2015.
50. Cun D, Foged C, Yang M, et al. Preparation and characterization of poly(dl-lactide-co-glycolide) nanoparticles for siRNA delivery. International Journal of Pharmaceutics 2010;390:70-75.
51. Palmer TD, Ashby WJ, Lewis JD, et al. Targeting tumor cell motility to prevent metastasis. Adv Drug Deliv Rev 2011;63:568-81.
52. Zhang H, Lu H, Xiang L, et al. HIF-1 regulates CD47 expression in breast cancer cells to promote evasion of phagocytosis and maintenance of cancer stem cells. Proc Natl Acad Sci U S A 2015;112:E6215-23.
53. Liu ZJ, Semenza GL, Zhang HF. Hypoxia-inducible factor 1 and breast cancer metastasis. J Zhejiang Univ Sci B 2015;16:32-43.
54. Chaturvedi P, Gilkes DM, Takano N, et al. Hypoxia-inducible factor-dependent signaling between triple-negative breast cancer cells and mesenchymal stem cells promotes macrophage recruitment. Proc Natl Acad Sci U S A 2014;111:E2120-9.

55. Patel SA, Simon MC. Biology of hypoxia-inducible factor-2alpha in development and disease. Cell Death Differ 2008;15:628-34.
56. Shukla S, MacLennan GT, Fu P, et al. Nuclear factor-kappaB/p65 (Rel A) is constitutively activated in human prostate adenocarcinoma and correlates with disease progression. Neoplasia 2004;6:390-400.
57. Bollu VS, Barui AK, Mondal SK, et al. Curcumin-loaded silica-based mesoporous materials: Synthesis, characterization and cytotoxic properties against cancer cells. Materials Science and Engineering: C 2016;63:393-410.
58. Pandit RS, Gaikwad SC, Agarkar GA, et al. Curcumin nanoparticles: physico-chemical fabrication and its in vitro efficacy against human pathogens. 3 Biotech 2015;5:991-997.
59. Tiwari SK, Agarwal S, Seth B, et al. Curcumin-loaded nanoparticles potently induce adult neurogenesis and reverse cognitive deficits in Alzheimer's disease model via canonical Wnt/beta-catenin pathway. ACS Nano 2014;8:76-103.
60. Yallapu MM, Khan S, Maher DM, et al. Anti-cancer activity of curcumin loaded nanoparticles in prostate cancer. Biomaterials 2014;35:8635-48.
61. Anitha A, Deepa N, Chennazhi KP, et al. Combinatorial anticancer effects of curcumin and 5-fluorouracil loaded thiolated chitosan nanoparticles towards colon cancer treatment. Biochim Biophys Acta 2014;1840:2730-43.
62. Wang P, Zhang L, Peng H, et al. The formulation and delivery of curcumin with solid lipid nanoparticles for the treatment of on non-small cell lung cancer both in vitro and in vivo. Mater Sci Eng C Mater Biol Appl 2013;33:4802-8.
63. Chang PY, Peng SF, Lee CY, et al. Curcumin-loaded nanoparticles induce apoptotic cell death through regulation of the function of MDR1 and reactive oxygen species in cisplatin-resistant CAR human oral cancer cells. Int J Oncol 2013;43:1141-50.
64. Yallapu MM, Ebeling MC, Khan S, et al. Novel curcumin-loaded magnetic nanoparticles for pancreatic cancer treatment. Mol Cancer Ther 2013;12:1471-80.
65. Verderio P, Bonetti P, Colombo M, et al. Intracellular drug release from curcumin-loaded PLGA nanoparticles induces G2/M block in breast cancer cells. Biomacromolecules 2013;14:672-82.
66. Punfa W, Yodkeeree S, Pitchakarn P, et al. Enhancement of cellular uptake and cytotoxicity of curcumin-loaded PLGA nanoparticles by conjugation with anti-P-glycoprotein in drug resistance cancer cells. Acta Pharmacol Sin 2012;33:823-31.
67. Rejinold NS, Muthunarayanan M, Chennazhi KP, et al. Curcumin loaded fibrinogen nanoparticles for cancer drug delivery. J Biomed Nanotechnol 2011;7:521-34.

Figure captions

Figure 1. Effect of polymer amount on particle size, zeta potential, encapsulation efficiency and *in-vitro* release

The particle size of nanoparticles increases significantly as the polymer amount increases from 30 mg to 90 mg (A). Zeta potential decreases significantly (p-value < 0.002) upon increasing the polymer amount from 30 mg to 90 mg (B). Entrapment efficiency increases with increase in PLGA amount (C). The release profile depicts initial burst release after 24 hours. Nanoparticles formulated using 60 mg PLGA shows the highest percentage release of curcumin (D). Values are mean ± SEM (n = 3). *p < 0.05, **p < 0.01 and ***p < 0.001 compared with 30 mg PLGA. Δp < 0.05 and ΔΔΔp < 0.001 compared with 60 mg of PLGA.

Figure 2. Water solubility of cur-PLGA-NP, free curcumin and UV-spectra of cur-PLGA-NP and free curcumin.

The vials in Figure A shows the solubility of cur-PLGA-NP and free curcumin respectively. The free curcumin precipitates and settles down whereas cur-PLGA-NP shows uniform dispersion throughout the vial. Figure B shows the absorption spectra of cur-PLGA-NP and free curcumin. cur-PLGA-NP shows the greater area under the curve as compared to free curcumin in Figure B.

Figure 3. Scanning Electron Microscopy of cur-PLGA-NP F1, F2, and F3 containing 30 mg, 60 mg and 90 mg of PLGA polymer respectively.

Scanning electron microscopic images of F1, F2 and F3 batches containing 30 mg, 60 mg and 90 mg of PLGA demonstrate an increase in particle size. F1 has smaller and uniform particle size as compared to F2 and F3. SEM images confirm that increase in polymer amount leads to increase in particle size and distortion of particle shape.

Figure 4. Cellular Uptake of cur-PLGA-NP in MDA-MB231.

Cellular localisation of Nile red-coated cur-PLGA-NP were observed in MDA-MB231 (A) and A549 (B) and visualised by overlapping under fluorescent microscopy.

Figure 5. Effect of cur-PLGA-NP and free curcumin on the migration of MDA-MB231 and A549 cell lines.

The effect of cur-PLGA-NP and free curcumin on migration capacity of MDA-MB231 (A) and A549 (B) cell lines were evaluated. Cur-PLGA-NP shows significant reduction in migration capability of both cell lines as compared to free curcumin. Values are mean ± SEM with n=3. *P<0.05, **P<0.01, ***P<0.001 compared with control (blank NP). ΔP<0.05, ΔΔ P<0.01, ΔΔΔP<0.001 compared with the same dose of free curcumin.

Figure 6. Effect of cur-PLGA-NP and free curcumin on invasion of MDA-MB231 and A549 cell lines.

The effect of cur-PLGA-NP and free curcumin on invasion capability of MDA-MB231 (A) and A549 (B) cell lines was observed. Cur-PLGA-NP shows a significant reduction in invasion capability of both cell lines as compared to free curcumin. Values are mean ± SEM with n=3. *P<0.05, **P<0.01, ***P<0.001 compared with control (blank NP). ΔP<0.05, ΔΔ P<0.01, ΔΔΔP<0.001 compared with the same dose of free curcumin.

Figure 7. Effect of cur-PLGA-NP and free curcumin on colony formation ability of MDA-MB231 and A549 cell lines.

Cur-PLGA-NP significantly reduces the colony formation ability of both MDA-MB231 (A) and A549 (B) cell lines. Cur-PLGA-NP shows a significant reduction in colony formation capability of both cell lines as compared to free curcumin. Values are mean ± SEM with n=3. *P<0.05, **P<0.01, ***P<0.001 compared with control (blank NP). ΔP<0.05, ΔΔ P<0.01, ΔΔΔP<0.001 compared with the same dose of free curcumin.

Figure 8. Effect of cur-PLGA-NP and free curcumin on expression of cellular levels of HIF-1α and p65 (Rel A).

Cur-PLGA-NP significantly reduces the levels of HIF-1α (A) and p65 (Rel A) (B) in both MDA-MB231 and A549 cell lines. Values are mean ± SEM with n=4. **P<0.01, ***P<0.001 compared with blank NP. ΔΔ P<0.01, ΔΔΔP<0.001 compared with the same dose of free curcumin treatment for 24 hours.

Supplementary Figure 1. The level of HIF-1α and p65 in MDA-MB-231 and A549 at normal atmospheric (21%) O2 level.

Supplementary Figure 2. Cytotoxicity of cur-PLGA-NP and raw curcumin in MDA-MB231 and A549 cell lines

Cytotoxicity was performed on MDA-MB231 (A) and A549 (B) cell lines. 40×104 cells were seeded on 24-well plates and transfected with 10μM, 20μM and 30μM of raw curcumin and cur-PLGA-NP. The absorbance was measured after 24 hours, 48 hours, 72 hours and 96 hours. It is evident from the figures that cur-PLGA-NP have higher cellular viability and less cytotoxicity as compare to raw curcumin. Values are mean ± SEM (n = 3).

Figure 1.

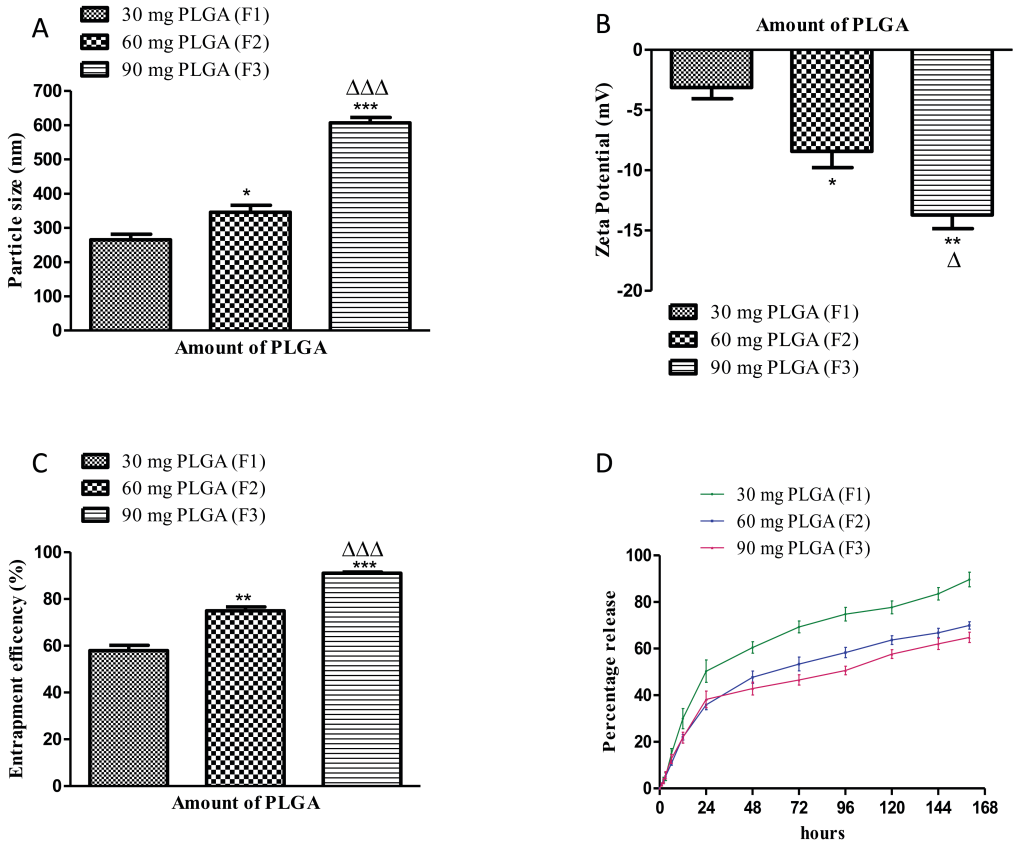
A
30 mg PLGA (F1)
60 mg PLGA (F2)
90 mg PLGA (F3)
Particle size (nm)
Amount of PLGA
ΔΔΔ
***
*
B
Amount of PLGA
Zeta Potential (mV)
*
**
Δ
30 mg PLGA (F1)
60 mg PLGA (F2)
90 mg PLGA (F3)
C
30 mg PLGA (F1)
60 mg PLGA (F2)
90 mg PLGA (F3)
Entrapment efficency (%)
Amount of PLGA
ΔΔΔ
***
**
D
30 mg PLGA (F1)
60 mg PLGA (F2)
90 mg PLGA (F3)
Percentage release
hours

Figure2.

A

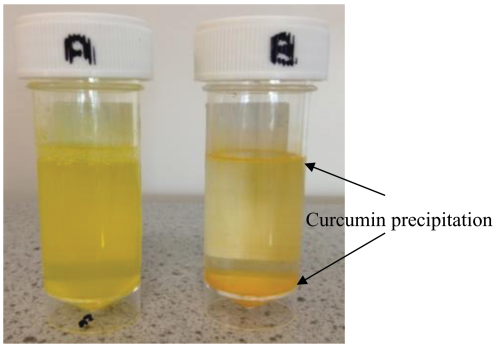
Curcumin precipitation

B

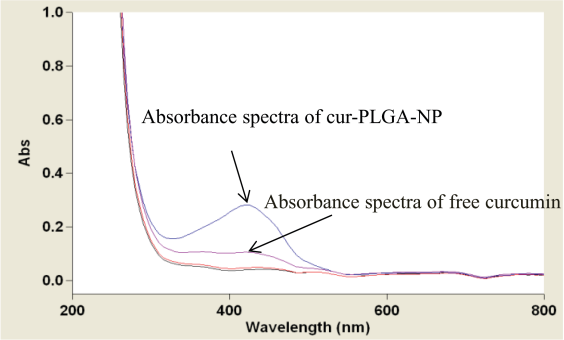
1.0
0.8
0.6
0.4
0.2
0.0
Abs
Absorbance spectra of cur-PLGA-NP
Absorbance spectra of free curcumin
200
400
600
800
Wavelength (nm)

Figure 3.

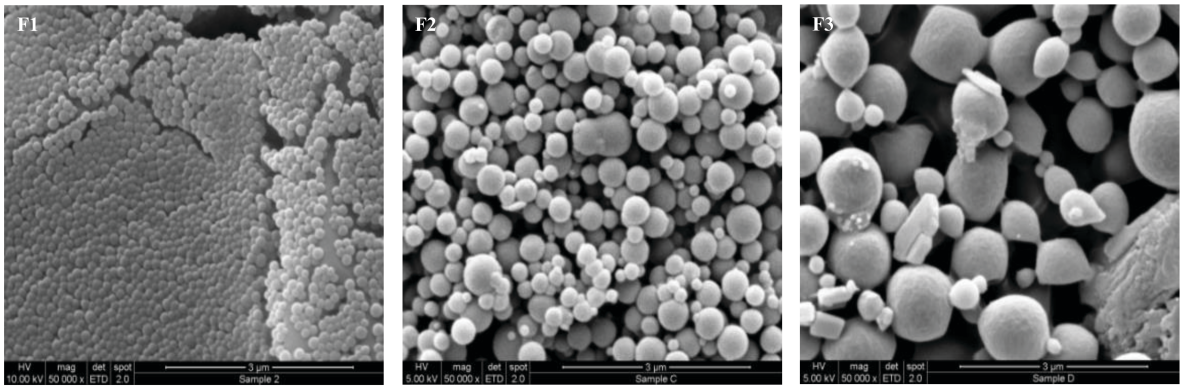
F1
HV mag det spot
10.00 kV 50 000 x ETD 2.0
3 µm
Sample 2
F2
HV mag det spot
5.00 kV 50 000 x ETD 2.0
3 µm
Sample C
F3
HV mag det spot
5.00 kV 50 000 x ETD 2.0
3 µm
Sample D

Figure 4.

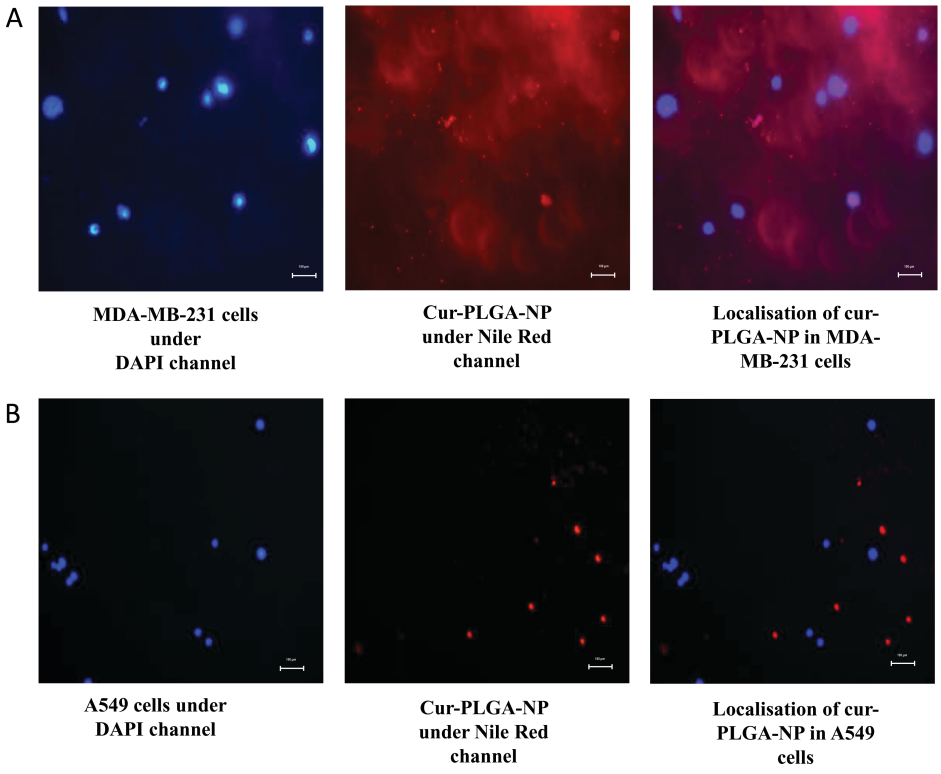
A
MDA-MB-231 cells under DAPI channel
Cur-PLGA-NP under Nile Red channel
Localisation of cur-PLGA-NP in MDA-MB-231 cells
B
A549 cells under DAPI channel
Cur-PLGA-NP under Nile Red channel
Localisation of cur-PLGA-NP in A549 cells

Figure 5.

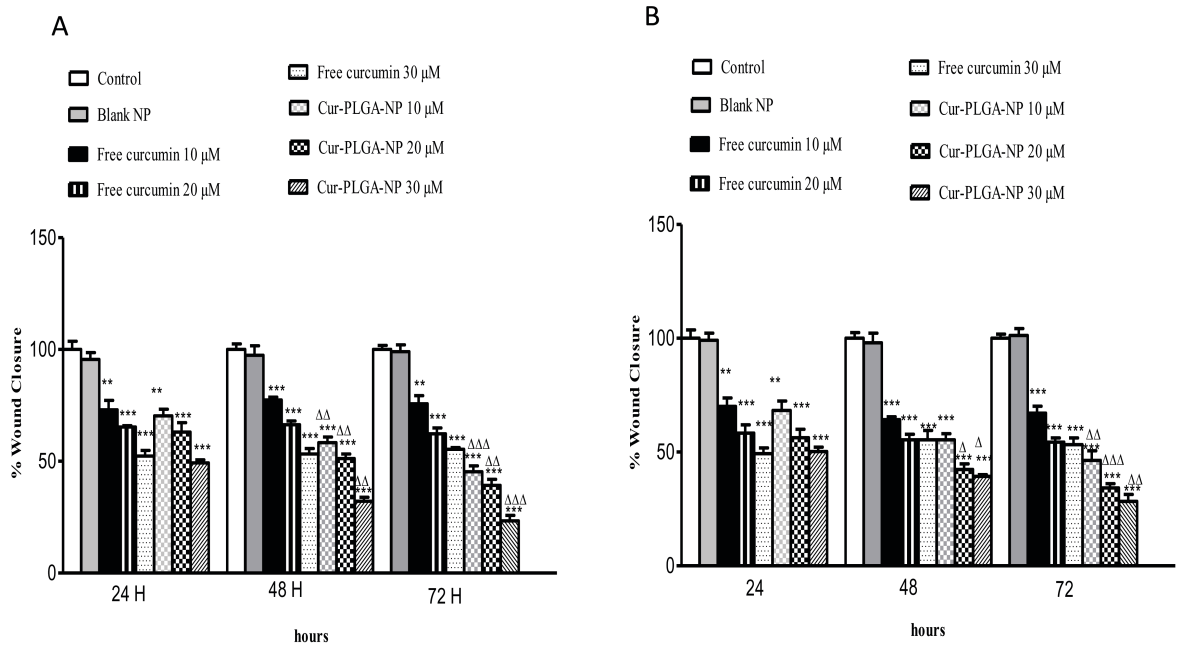
A
Control
Blank NP
Free curcumin 10 µM
Free curcumin 20 µM
Free curcumin 30 µM
Cur-PLGA-NP 10 µM
Cur-PLGA-NP 20 µM
Cur-PLGA-NP 30 µM
% Wound Closure
150
100
50
0
24 H
48 H
72 H
hours
B
Control
Blank NP
Free curcumin 10 µM
Free curcumin 20 µM
Free curcumin 30 µM
Cur-PLGA-NP 10 µM
Cur-PLGA-NP 20 µM
Cur-PLGA-NP 30 µM
% Wound Closure
150
100
50
0
24
48
72
hours

Figure 6.

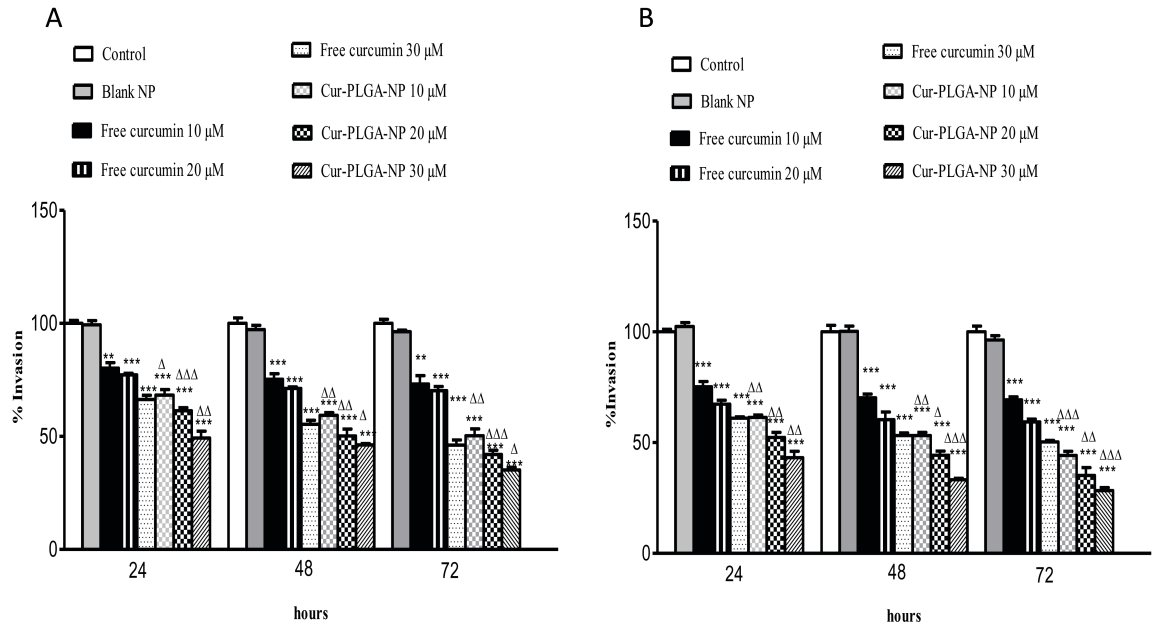
A
Control
Blank NP
Free curcumin 10 μM
Free curcumin 20 μM
Free curcumin 30 μM
Cur-PLGA-NP 10 μM
Cur-PLGA-NP 20 μM
Cur-PLGA-NP 30 μM
% Invasion
150
100
50
0
24
48
72
hours
B
Control
Blank NP
Free curcumin 10 μM
Free curcumin 20 μM
Free curcumin 30 μM
Cur-PLGA-NP 10 μM
Cur-PLGA-NP 20 μM
Cur-PLGA-NP 30 μM
%Invasion
150
100
50
0
24
48
72
hours

Figure 7.

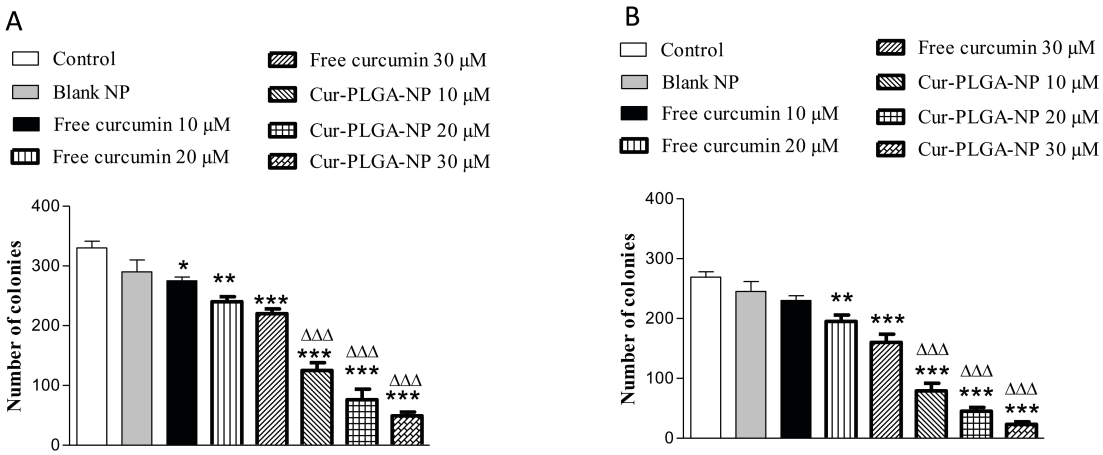
A
Control
Blank NP
Free curcumin 10 μM
Free curcumin 20 μM
Free curcumin 30 μM
Cur-PLGA-NP 10 μM
Cur-PLGA-NP 20 μM
Cur-PLGA-NP 30 μM
Number of colonies
400
300
200
100
0
*
**
***
ΔΔΔ
***
ΔΔΔ
***
ΔΔΔ
***
B
Control
Blank NP
Free curcumin 10 μM
Free curcumin 20 μM
Free curcumin 30 μM
Cur-PLGA-NP 10 μM
Cur-PLGA-NP 20 μM
Cur-PLGA-NP 30 μM
Number of colonies
400
300
200
100
0
**
***
ΔΔΔ
***
ΔΔΔ
***
ΔΔΔ
***

Figure 8.

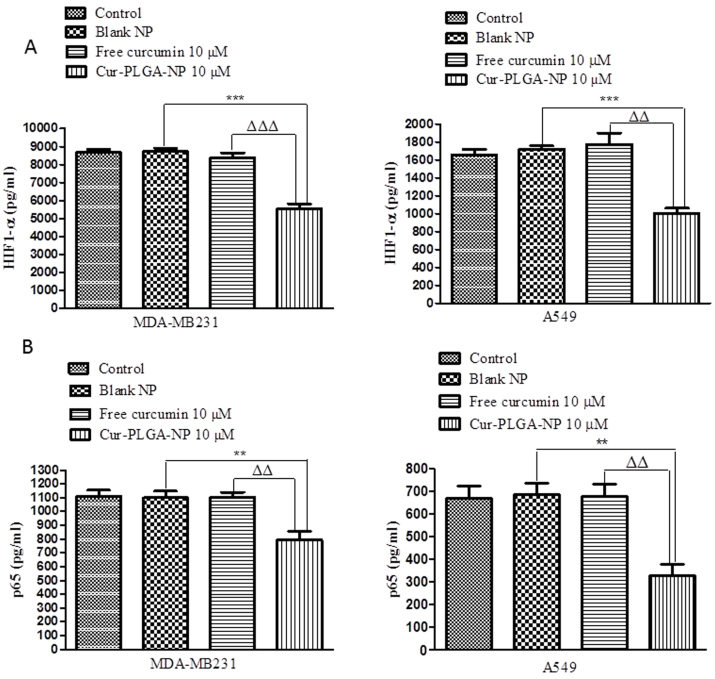
A
Control
Blank NP
Free curcumin 10 μM
Cur-PLGA-NP 10 μM
HIF1-α (pg/ml)
MDA-MB231
A549
B
p65 (pg/ml)
MDA-MB231
A549

Supplementary Figure 1.

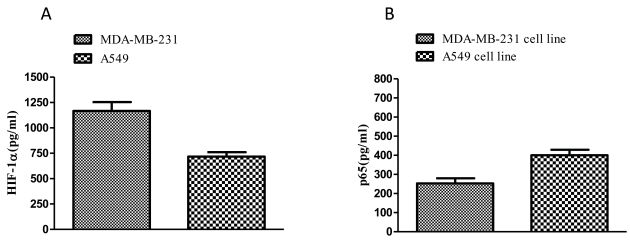

Supplementary Figure 2.

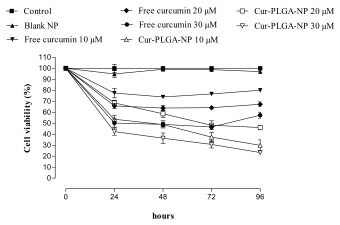

Table 1: Process variables for curcumin loaded NPs and corresponding identifiers.

Formulation code	Amount of drug (mg)	Amount of polymer (mg)
F1	20	30
F2	20	60
F3	20	90